

Insight into selectivity differences of glycerol electro-oxidation on Pt(111) and Ag(111)

Zhe Meng,^a David Tran,^b Johan Hjelm,^b Henrik H. Kristoffersen,^{*,a} and Jan Rossmeisl^a

^a Department of Chemistry, University of Copenhagen, Copenhagen 2100, Denmark

^b Department of Energy Conversion and Storage, Technical University of Denmark, Fysikvej 310, 2800 Kgs. Lyngby, Denmark

*E-mail: hhk@chem.ku.dk

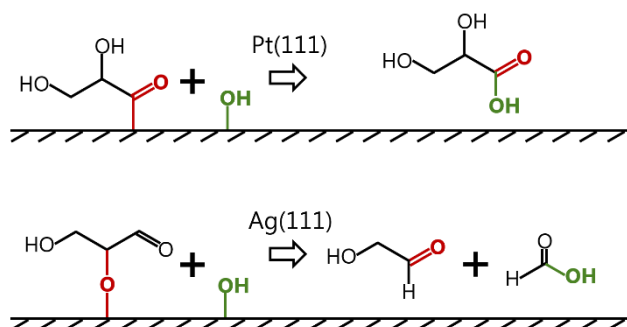
Abstract

Electro-oxidation is a way to utilize glycerol, a byproduct of biodiesel production, to produce fuels and feedstock chemicals for the chemical industry. A significant challenge is to get products with high selectivity, so it is desirable to understand the glycerol oxidation mechanisms in further details. Using density functional theory calculations, we investigate possible glycerol oxidation intermediates on Pt(111) and Ag(111). We find that the different adsorption preferences of the intermediates on Pt (adsorption via carbon atoms) and on Ag (adsorption via oxygen atoms) lead to different preferred reaction pathways, resulting in different products. The reaction pathways on both surfaces involve glyceraldehyde as a key intermediate, however, upon further oxidation, Pt(111) preferentially produces glyceric acid ($\text{CH}_2\text{OH-CHOH-COOH}$), while on Ag(111) C-C bonds are broken, which leads to production of glycolaldehyde and formic acid ($\text{CH}_2\text{OH-CHO}$ and HCOOH). These predictions agree well with the experimental outcome of electro-oxidation of glycerol on Pt and Ag surfaces. Our study therefore provides useful insights for optimizing the selectivity of glycerol oxidation and improving the utilization of glycerol.

Keywords:

Glycerol; oxidation; DFT calculations; selectivity; platinum, silver; electrocatalysis

TOC Graphic



1. Introduction

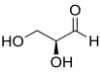
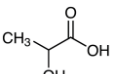
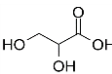
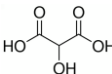
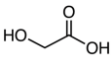
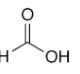
Glycerol is an abundant byproduct from biodiesel production,¹⁻³ which can be converted to sustainable value-added chemicals and fuels via electro-oxidation.⁴⁻⁶ However, additional research is required to understand the underlying reaction mechanisms and to optimize the reaction pathways on different electrocatalysts toward desired products.

In an attempt to understand the underlying reaction mechanisms, we start by recapping experimental glycerol electro-oxidation product selectivities on different metal surfaces and reaction conditions found in the literature (Table 1). We present an extended literature data collection in Table S2 in Supporting Information, which contains experimental data from ref ⁷⁻²⁰. Platinum is the most studied electrocatalyst for glycerol oxidations, so we can use the Pt data in Table 1 to establish a few overall principles. Firstly, increasing the electrode potential (vs the reversible hydrogen electrode (RHE)) shifts the glycerol oxidation selectivity from weakly to strongly oxidized products. More specifically, the dominant products shifts from glyceraldehyde (at less than 0.9 V vs RHE) to glyceric acid and tartronic acid (between 0.9 V and 1.2 V vs RHE), and finally to formic acid (at 1.44 V vs RHE).^{7,9,11-13} The formation of formic acid means that Pt is able to break C-C bonds, but only under very strong oxidizing conditions.¹¹ Secondly, when glyceraldehyde is produced under alkaline conditions, it quickly isomerizes in solution and turns into lactic acid.^{13,21} Thirdly, another way to favor more oxidized products is to lower the glycerol concentration. This is shown by the two experiments from ref ⁹, where the first experiment is conducted with 0.1 M glycerol and mostly yields glyceric acid, and the second experiment is conducted with 1 M glycerol and mostly yields glyceraldehyde.

Table 1 further shows that glycerol electro-oxidation on Au can give some of the same C3 products as on Pt, i.e., lactic acid and glyceric acid. However, Au can also break C-C bonds, resulting in noteworthy amounts of C2 (glycolic acid) and C1 (formic acid) products. The simultaneous

formation of C3, C2, and C1 reduces the overall glycerol electro-oxidation selectivity on Au. The last row in Table 1 shows the result of a glycerol electro-oxidation experiment on Ag. The rate of glycerol electro-oxidation on Ag is quite low, but importantly, the experiment reports very little C3 products and, instead, observe C2 (glycolic acid) and C1 (formic acid) products.¹⁶ This indicates that Ag has a strong preference for C-C bond breaking.²²

Table 1. Experimental product selectivities of electro-oxidation of glycerol on different metal catalysts and reaction conditions.

catalyst	GLAD 	LA 	GLA 	TA 	GLCA 	FA 	U_{vsRHE}	pH	ref
Pt/C	16					78	1.44	0	¹¹
			41	50			1.2	14.3	⁷
	20		67.3				0.9	0	⁹
	88.6		10.4				0.9	0	⁹
		22.6	50.0				0.9	14	¹³
	58.6		18.1				0.8	0	¹²
		50.4	41.6				0.45	14	¹³
	100						0.37	0	¹¹
Au/C			50.3		13.7		1.57	13	¹⁵
		44.5	14.7		11.9	24.4	0.9	14	¹³
Ag/C					37	61	~1	13.7	¹⁶

GLAD, glyceraldehyde; LA, lactic acid; GLA, glyceric acid; TA, tartronic acid; GLCA, glycolic acid;

FA, formic acid. For better overview, we only include product selectivities higher than 10%.

We believe that the C-C bond breaking preference of Ag compared to Pt is very interesting, especially if it can be explained by simple surface specific properties that differ for Ag and Pt. In this regard, the following theoretical studies are of special relevance. Firstly, the observed Pt product selectivities (Table 1) have been rationalized by DFT calculations of glycerol oxidation intermediates on Pt(111).²³ Secondly, a recent study found that glycerol adsorbs either via a carbon (C*) atom or an oxygen (O*) atom depending on the surface in question. Ag prefers glycerol adsorption via O*, while Pt prefers glycerol adsorption via C* atom.²⁴ Finally, a related study found that the glycerol adsorption energy is a good descriptor for the subsequent reaction steps.²⁵ Combining the insight from these studies, we hypothesize that the difference in adsorption preference of glycerol (and subsequent intermediates) is responsible for the difference in glycerol electro-oxidation products. In this paper, we therefore investigate the stability of possible glycerol electro-oxidation reaction intermediates and products on Pt(111) and Ag(111) with DFT calculations. Based on our results and the current scientific understanding, we propose the main reaction pathways shown in Figure 1 for glycerol electro-oxidation on Pt(111) and Ag(111). The first reaction step is glycerol adsorption via a C* atom on Pt(111) and via an O* atom on Ag(111). This and all other vertical reaction steps in Figure 1 release $H^+ + e^-$ and is therefore electrochemical in nature. The next step produces glyceraldehyde in both cases, even though the glycerol adsorbs differently on the two surfaces. As mentioned earlier, glyceraldehyde can undergo isomerization to lactic acid in alkaline solution (not electrochemical),^{13,21} however, if glyceraldehyde adsorbs, it will preferably bind via the aldehyde C* atom on Pt(111) and via the middle hydroxyl O* atom on Ag(111). The different adsorption configurations are crucial for how the next electro-oxidation step occurs, specifically the addition of OH. On Pt(111), the C* atom can concertedly break the bond to the surface, while simultaneously forming a bond to OH. This produces glyceric acid in good agreement with the experimental behavior of Pt (Table 1).

On Ag(111), OH forms a bond with the aldehyde C atom, which leads to the breaking of a C-C bond, and formation of glycolaldehyde and formic acid.

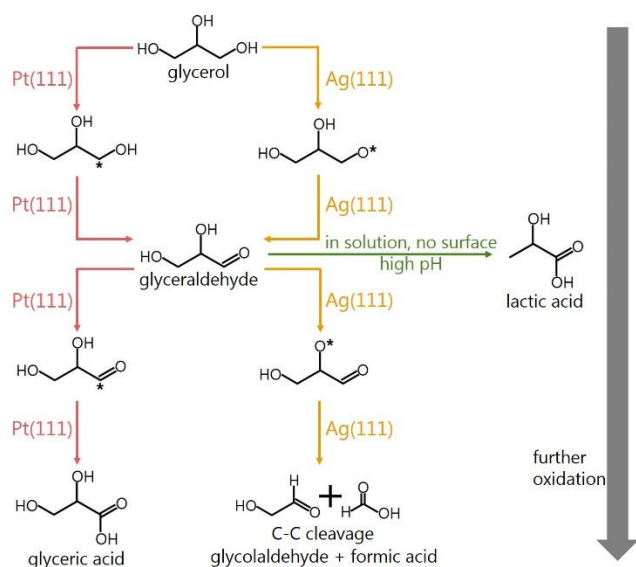


Figure 1. Proposed glycerol electro-oxidation pathways on Pt(111) and Ag(111).

2. Computational details

We have used density functional theory (DFT) to calculate energies of possible glycerol electro-oxidation intermediates and products. In our modeling, the intermediates are adsorbed on metal slabs with 4×4 (111) surface cells and four atomic layer thicknesses. We fix the two bottom layers of the slabs to emulate bulk metal and include 22 Å distance between metal slabs (periodic images) to avoid interlayer interactions. The atomic structures are set up with the atomic simulation environment (ASE) program.²⁶ The DFT calculations are carried out with the GPAW program^{27,28} using the revised Perdew-Burke-Ernzerhof (RPBE) exchange correlation functional,²⁹ plane-wave basis sets with 400 eV energy cut-off, and $4 \times 4 \times 1$ Monkhorst-Pack k-point sampling. The atomic structures are relaxed to a maximum force of 0.10 eV/Å on each atom. Finally, we use the climbing-image nudged elastic

band (NEB) method³⁰ to obtain activation energies for formation of glyceric acid and two competing intermediates in the fourth oxidation step on Pt(111).

We consider two types of reactions in order to elucidate the glycerol electro-oxidation pathways on Pt(111) and Ag(111). The first reaction type is dehydrogenation (eq 1), where one hydrogen is removed from the adsorbate ($C_3H_yO_x$) resulting in a more oxidized glycerol intermediate ($C_3H_{y-1}O_x$) and the transfer of $H^+(aq)$ to the electrolyte and e^- to the circuit.



The second reaction type is incorporation of OH (eq 2) into the adsorbate, which also results in a more oxidized glycerol intermediate ($C_3H_{y+1}O_{x+1}$), as well as consumption of one liquid H_2O molecule and formation of $H^+(aq) + e^-$.



Many computational studies have considered hydrogen removal starting from glycerol via reaction eq 1,^{24,25,31-33} while fewer studies have also considered OH addition via reaction eq 2.^{23,34,35}

The $H^+(aq)$ and e^- species are difficult to model, so we use the computational hydrogen electrode approach (eq 3),^{36,37} which connects the free energy of $H^+(aq)$ and e^- to the free energy of gas phase H_2 and the electrostatic potential at the RHE scale (U_{vsRHE}).

$$\Delta G(H^+(aq) + e^-) = \frac{1}{2} \Delta G(H_2) - eU_{vsRHE} \quad (3)$$

We set $U_{vsRHE} = 0$ throughout the Results and discussion section, but keep in mind that both types of electro-oxidation steps (eq 1 and eq 2) are stabilized by $-eU_{vsRHE}$ when applying $U_{vsRHE} > 0$.

We calculate the DFT energy differences of the adsorbed intermediates ($\Delta E_{intermediate}$) in the following way:

$$\Delta E_{intermediate} = E_{slab+intermediate} - E_{slab} - E_{glycerol} + n_{H_2}E_{H_2} - m_{H_2O}E_{H_2O} \quad (4)$$

In eq 4, $E_{slab+intermediate}$ and E_{slab} represent the DFT energy of the slab with and without adsorbed intermediates, respectively, while $E_{glycerol}$, E_{H_2} , and E_{H_2O} represent the DFT energies of gas phase glycerol, gas phase H_2 , and gas phase H_2O , respectively. n_{H_2} is the total number of produced hydrogen molecules and m_{H_2O} is the total number of consumed H_2O molecules, when converting glycerol to the intermediate in question.

The $\Delta E_{intermediate}$ values do not include entropy differences, zero-point energy differences, or heating enthalpy differences, which are needed to convert DFT reaction energies to reaction free energies. The size of these effects has been mapped out in the literature for CH_3O^* reduction to $COOH^*$.³⁸ This reduction goes through three type eq 1 reaction steps with an average free energy correction of $\Delta G_{eq1}^{corr} = -0.32\text{eV}$ (standard deviation of 0.06 eV), and one type eq 2 reaction step with a free energy correction of $\Delta G_{eq2}^{corr} = +0.39\text{eV}$ (details are included in the Supporting Information). We adopt the same free energy corrections, even though we study glycerol reduction instead of methanol reduction, and approximated the free energy differences of the adsorbed intermediates $\Delta G_{intermediate}$ by eq 5. The n_{eq1} and m_{eq2} in eq 5 are the number of eq 1 and eq 2 reaction steps needed to convert glycerol to the intermediate in question.

$$\Delta G_{intermediate} = \Delta E_{intermediate} + n_{eq1}\Delta G_{eq1}^{corr} + m_{eq2}\Delta G_{eq2}^{corr} \quad (5)$$

The corrections use gas phase H_2O pressure of 0.0035 MPa, such that the free energy of gas phase H_2O is the same as the free energy of liquid H_2O , since liquid H_2O is the relevant species in room temperature electrochemistry.³⁶ We note that our calculations do not account for solvation of the glycerol molecule and subsequent reaction intermediates nor do we impose constant potential at the interface. Solvation effects can be especially large, but unfortunately, they are also prohibitively computationally expensive to accurately account for.³⁹

The fourth oxidation step incorporates OH into the glycerol oxidation intermediates via eq 2 on both Pt(111) and Ag(111). This likely requires that both the OH and the intermediate are adsorbed on the surface. This is supported by glycerol electro-oxidation on Au(111), where adsorbed *OH is found to be the oxidative species under alkaline conditions.⁴⁰ In the fourth oxidation step, we therefore also consider the free energy of the following *OH formation reaction (eq 6).



The computed reaction free energy of eq 6 is $\Delta G = 1.40$ eV on Pt(111) at $U_{\text{vsRHE}} = 0$ (using the 0.37 eV free energy correction associated with eq 2). However, we know from experiments that this is erroneous and should be around $\Delta G = 0.76$ eV.⁴¹ The error is largely due to us neglecting solvation of the *OH species.⁴² We therefore use experimental insight, rather than calculations, to set $\Delta G = 0.76$ eV for *OH formation on Pt(111)⁴³ and use the calculated *OH adsorption energy difference between Pt(111) and Ag(111) to obtain $\Delta G = 0.48$ eV for Ag(111).

The DFT calculations and python scripts, which form the basis of this study, are accessible online at <https://nano.ku.dk/english/research/theoretical-electrocatalysis/katldb/glycerol-electro-oxidation>.

3. Results and discussion

Glycerol adsorbs electrochemically on metal surfaces by releasing a H atom in the form of H^+ and e^- . Following the approach of^{24,25}, we have compared glycerol adsorption free energies for adsorption via C* and adsorption via O* and present our results in Figure 2. Similar to the previous studies, we find that Pt(111) and Pd(111) have preference for glycerol adsorption via a C* atom, while Ag(111), Cu(111), and Ru(111) have strong preference for glycerol adsorption via an O* atom. Au(111) equally prefers adsorption via either O* or C* atom. The preference for O* or C* adsorption is controlled by the electronic structure of the metal in question. The relations between adsorption strength and

electronic structure have been extensively studied in the literature, for instance for *OH and *CH₃ in ⁴⁹ and for O* and *CO in ⁴⁴. It is therefore well established that some metals (e.g. Ag and Cu) prefer adsorption via O* atoms, whereas other metals (e.g. Pt and Pd) prefer adsorption via C* atoms.

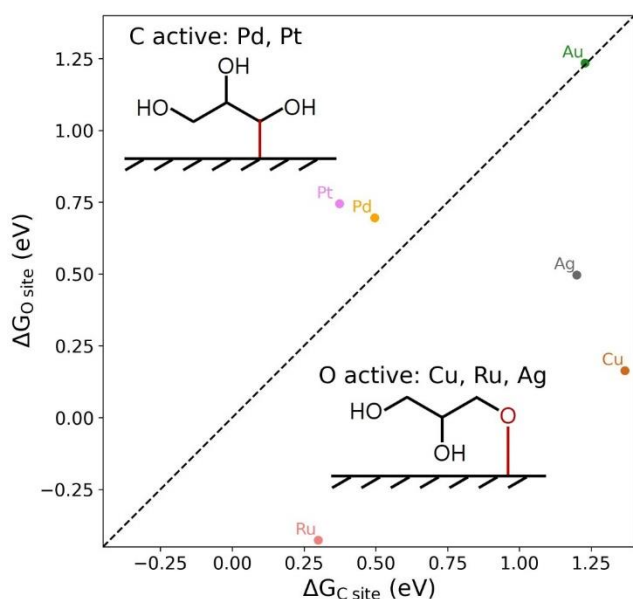


Figure 2. The Gibbs free energy difference for glycerol adsorption ($C_3H_8O_3(g) \rightarrow C_3H_7O_3^* + \frac{1}{2}H_2(g)$) via C* adsorption ($\Delta G_{C \text{ site}}$) vs O* adsorption ($\Delta G_{O \text{ site}}$) on (111) metal surfaces.

Our hypothesis is that the preference for C* or O* adsorption on different catalyst surfaces is responsible for glycerol electro-oxidation product selectivity. We test this by modeling and comparing glycerol electro-oxidation on Pt(111), which prefers glycerol adsorption via C*, to electro-oxidation on Ag(111), which prefers glycerol adsorption via O*. At every oxidation step, we look for the most stable intermediate obtained by reaction eq 1 or reaction eq 2, and (with a rationalized exception for glyceraldehyde on Pt(111)) use this intermediate as the reactant for the next oxidation step. This maps out the reaction diagram illustrated in Figure 1 and the free energy landscape shown in Figure 3. Our

reaction pathway on Pt(111) is similar to the one presented in ref ²³, which is also based on DFT calculations.

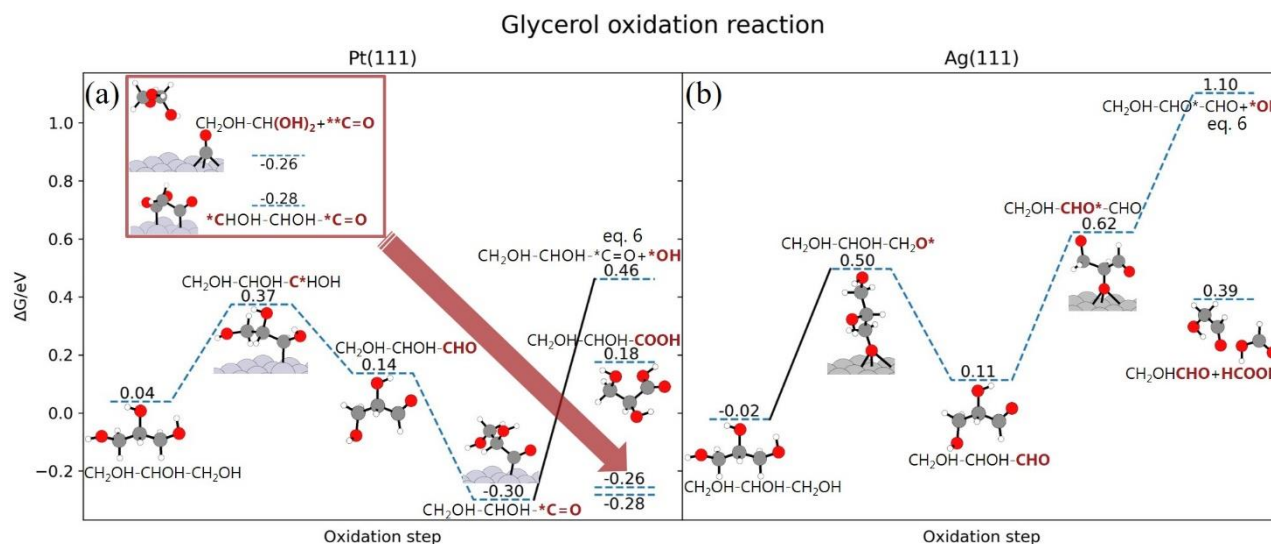


Figure 3. Free energy landscape for glycerol electro-oxidation on Pt(111) and Ag(111). Atom color code, red: O; grey: C; white: H. We highlight the potential determining step with a solid black line.

We now discuss the oxidation steps shown in Figure 3, one by one. Initially, glycerol is physisorbed on Pt(111) and Ag(111) with adsorption free energies of 0.04 eV and -0.02 eV, respectively, compared to gas phase glycerol. In the *first oxidation step*, a H atom is removed and glycerol is chemisorbed via a C* atom on Pt(111) and via an O* atom on Ag(111) with adsorption free energies of 0.37 eV and 0.50 eV, respectively.

We propose that glyceraldehyde (CH₂OH-CHOH-CHO) formation by removal of another H atom is the most facile *second oxidation step* on both Pt(111) and Ag(111). On Pt(111), two intermediates ($\Delta G = 0.06$ eV, Figure 4a and $\Delta G = 0.07$ eV, Figure 4b) are more stable than glyceraldehyde ($\Delta G = 0.14$ eV, Figure 4c). These two intermediates remain on the surface and have

formed an additional bond to the Pt(111) surface by removing a H atom. The additional bond is either a new bond between the middle C atom and the surface (Figure 4a), or conversion of the existing bond between the end C atom and the surface into a double bond (Figure 4b). The fact that glyceraldehyde is observed in experimental glycerol electro-oxidation on Pt at ≤ 0.9 V vs RHE^{9,11,12} strongly indicate that the 0.08 eV additional free energy cost does not prohibit glyceraldehyde formation. The reason that our results do not predict glyceraldehyde formation could be kinetic (i.e. glyceraldehyde formation may have the lowest activation energy) or because we are missing important effect in our calculations, such as competitive adsorption between surface intermediates and water molecules^{45,46} or related to free energy differences between adsorbed and solvated species.⁴⁷ On Ag(111), glyceraldehyde is the most stable intermediate (Figure 4d) with $\Delta G = 0.11$ eV, which is significantly lower than the second ($\Delta G = 0.83$ eV, Figure 4e) and third ($\Delta G = 1.16$ eV, Figure 4f) most stable identified intermediate.

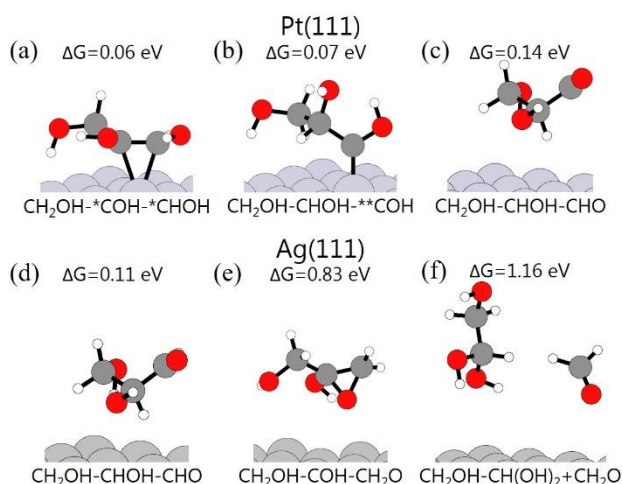


Figure 4. (a), (b), and (c) show the most stable C₃H₆O₃ or C₃H₈O₄ intermediates following oxidation of CH₂OH-CHOH-*CHOH on Pt(111). (d), (e), and (f) show the most stable C₃H₆O₃ or C₃H₈O₄ intermediates following oxidation of CH₂OH-CHOH-CH₂O* on Ag(111). The free energies of the

intermediates are in relation to gas phase glycerol, H₂O(l) and H₂(g). We report free energies and structures of all studied intermediates in Table S4 of the Supporting Information.

We examine glyceraldehyde re-adsorption in the *third oxidation step*. Similar to glycerol, glyceraldehyde adsorbs differently on the two surfaces when removing one H atom. On Pt(111), glyceraldehyde adsorbs via the aldehyde C* atom ($\Delta G = -0.30$ eV, Figure 5a). This CH₂OH-CHOH-*C=O configuration is significantly more stable than adsorption via the middle C* atom ($\Delta G = 0.20$ eV, Figure 5b), and adsorption via the last C* atom ($\Delta G = 0.39$ eV, Figure 5c). The glyceraldehyde adsorption step is also significantly more energetically favorable than the initial glycerol adsorption step. On Ag(111), the most stable intermediate is adsorbed via the middle hydroxyl O* atom ($\Delta G = 0.62$ eV, Figure 5d). This CH₂OH-CHO*-CHO configuration is only slightly more stable than adsorption via the last hydroxyl O* atom ($\Delta G = 0.65$ eV, Figure 5e), but more stable than adsorption via the middle C* atom ($\Delta G = 0.84$ eV, Figure 5f). Glyceraldehyde adsorption and the initial glycerol adsorption are equally energetically costly on Ag(111).

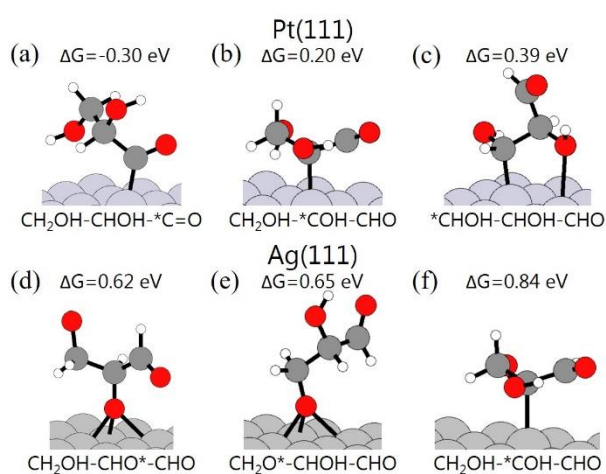


Figure 5. (a), (b), and (c) show the most stable $C_3H_5O_3^*$ intermediates on Pt(111) and (d), (e), and (f) show the most stable $C_3H_5O_3^*$ intermediates on Ag(111) following oxidation of glyceraldehyde ($CH_2OH-CHOH-CHO$). The free energies of the intermediates are in relation to gas phase glycerol, $H_2O(l)$ and $H_2(g)$. We report free energies and structures of all studied intermediates in Table S5 of the Supporting Information. We have not considered formation of $C_3H_7O_4^*$ intermediates, because this is an adsorption reaction (of glyceraldehyde).

Finally, we discuss the *fourth oxidation step*, which is also the last step we investigated. We find that on Pt(111) formation of glyceric acid has the lowest activation energy, explaining the high selectivity towards glyceric acid observed in experiments.^{7,9,13} However, Figure 6 shows that glyceric acid is not the most stable intermediate on Pt(111) following oxidation of $CH_2OH-CHOH-^*C=O$ (Figure 5a). Instead, it is more energetically favorable to remove a H atom from the last C atom to form $^*CHOH-CHOH-^*C=O$ that has an additional bond to the surface ($\Delta G = -0.28$ eV, Figure 6a). It is also more energy favorable to react OH with the middle C atom in $CH_2OH-CHOH-^*C=O$, which forms $CH_2OH-CH(OH)_2$, breaks a C-C bond, and leaves *CO on the surface ($\Delta G = -0.26$ eV, Figure 6b) and to remove a H atom from the middle C to form $CH_2OH-^*COH-^*C=O$ ($\Delta G = -0.26$ eV, shown in Table S6 of the Supporting Information). The formation of glyceric acid by addition of OH to aldehyde C* atom is only the fourth most stable intermediate ($\Delta G = 0.18$ eV, Figure 6c). However, NEB calculations show that glyceric acid formation is the most facile reaction, because it has the lowest activation energy.

We have started all the NEB calculations with *OH and $CH_2OH-CHOH-^*C=O$ on the surface. Since we compare very similar reactions, and are mainly interested in which reaction has the lower

barrier, it is also less problematic that we do not include solvation and constant potential effects in our NEB calculations.

The NEB reaction path from $*OH + CH_2OH-CHOH-*C=O$ to $*CHOH-CHOH-*C=O + H_2O*$ is shown in Figure 6d. We included $*OH$ in the NEB study to more fairly compare with the other NEB reaction paths. However, the obtained reaction path shows that the $*OH$ species does not facilitate the formation of the $*CHOH-CHOH-*C=O$ intermediate. Instead, the bond between the H atom and the last C atom is broken with the help of a surface Pt atom, forming a C^*-Pt bond and transferring the H atom to the surface. The $*OH$ species then reacts with H^* to form H_2O^* . The activation energy for the reaction is 1.07 eV, which is very close to the activation energy obtained without the presence of the $*OH$ species on the surface (1.00 eV, Figure S2a in the Supporting Information).

The NEB reaction path from $*OH + CH_2OH-CHOH-*C=O$ to $CH_2OH-CH(OH)_2$ and $*CO$ shows that addition of $*OH$ to the middle C atom does not happen in a concerted reaction (Figure 6e). Instead, the C-C bond is broken first, which leaves $*CO$ on the surface and only afterwards does $*OH$ react with the middle C atom. The lack of a concerted reaction results in a large activation energy of 0.96 eV.

Lastly, the formation of glyceric acid by $*OH$ addition to aldehyde C^* atom happens in a concerted reaction, where the C-OH bond is formed at the same time as the C-Pt bond is broken (Figure 6f). This results in a small activation energy of 0.48 eV, even though it has the least stable reaction energy of the investigated reaction pathways.

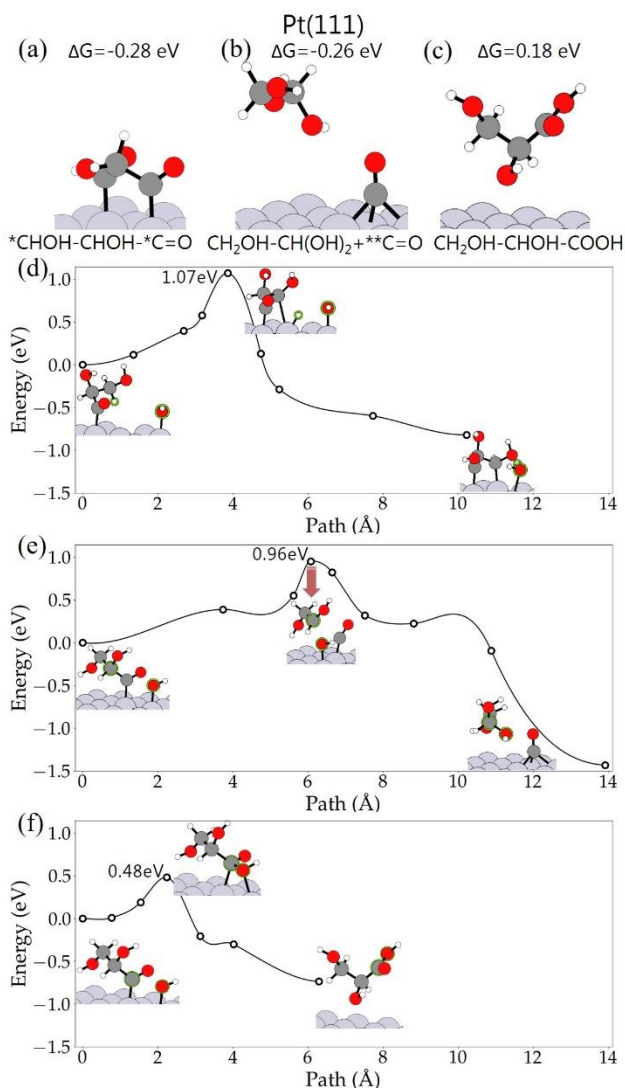


Figure 6. (a), (b) and (c) shows the most stable C₃H₄O₃ or C₃H₆O₄ intermediates following oxidation of CH₂OH-CHOH-*C=O (Figure 5a) on Pt(111). The CH₂OH-*COH-*C=O intermediate (not shown) has $\Delta G = -0.26$ eV on Pt(111). The free energies of the intermediates are in relation to gas phase glycerol, H₂O(l) and H₂(g). We report free energies and structures of all studied intermediates in Table S6 of the Supporting Information. NEB potential energy surfaces for (d) CH₂OH-CHOH-*C=O + *OH → *CHOH-CHOH-*C=O + H₂O* (e) CH₂OH-CHOH-*C=O + *OH → CH₂OH-CH(OH)₂ + *C=O and (f) CH₂OH-CHOH-*C=O + *OH → CH₂OH-CHOH-COOH on Pt(111). Inserts show structures of initial states, transition states, and final states for these reactions.

The most stable intermediate in the *fourth oxidation step* on Ag(111) is the combination of formic acid (HCOOH) and glycolaldehyde (CH₂OH-CHO) (Figure 7a), which is formed by the reaction between CH₂OH-CHO*-CHO (Figure 5d) and *OH. In the reaction, OH forms a bond with the aldehyde C atom, the aldehyde C atom breaks its bond to the middle C atom forming formic acid, and the middle C atom makes a double bond with the O* atom forming glycolaldehyde. The preference of Ag(111) to bind intermediates via O* atoms is therefore directly linked the preference for breaking C-C bonds in the intermediates. The formic acid and glycolaldehyde products also fits well with the main experimental products on Ag (formic acid and glycolic acid),¹⁶ given that glycolaldehyde can probably oxidize further, for instance to glycolic acid. The second and third most stable intermediates on Ag(111) have both lost a H atom to form a ketone on the middle C atom ($\Delta G = 0.53$ eV, Figure 7b), or a new bond between the aldehyde C atom and the surface ($\Delta G = 1.17$ eV, Figure 7c).

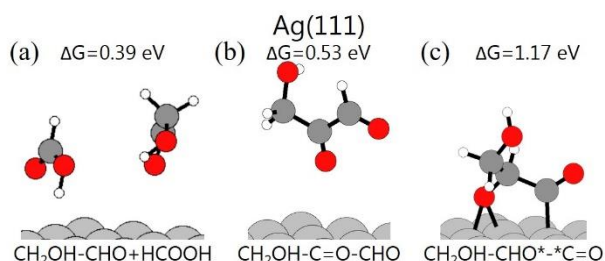


Figure 7. (a), (b), and (c) show the most stable C₃H₄O₃ or C₃H₆O₄ intermediates following oxidation of CH₂OH-CHO*-CHO (Figure 5d) on Ag(111). The free energies of the intermediates are in relation to gas phase glycerol, H₂O(l) and H₂(g). We report free energies and structures of all studied intermediates in Table S6 of the Supporting Information.

Our results for glycerol electro-oxidation on Pt(111) indicate that glyceraldehyde can be formed without the involvement of adsorbed *OH species, since all steps to glyceraldehyde happen via reaction eq 1. Additionally, the most costly oxidation step towards glyceraldehyde is adsorption of glycerol, which has $\Delta G = 0.37$ eV compared to gas phase glycerol (Figure 3). It therefore makes sense that glyceraldehyde (and lactic acid from glyceraldehyde isomerization) are the main products observed on Pt at low electrochemical potentials (≤ 0.9 V vs RHE).^{9,11-13} Adsorbed *OH species are required to oxidize glyceraldehyde to glyceric acid. We estimate that *OH formation has ΔG of 0.76 eV (based on experiments), which would make *OH formation the potential determining step in glyceric acid formation. The shift to glyceric acid and tartronic acid observed in experiments (between 0.9 V and 1.2 V vs RHE) on Pt, therefore fits very well with the potential region where *OH is available on the Pt surface.⁴⁸

On Ag(111), the 0.52 eV energy difference between physisorbed and chemisorbed glycerol makes this step potential determining (Figure 3). I.e. at 0.52 V vs RHE the $-eU_{vsRHE}$ stabilization from eq. 3 makes all steps downhill on Ag(111) including formation of *OH on the surface. The early potential determining step could be the reason that only very oxidized products (glycolic acid and formic acid) are reported in ref¹⁶, while the less stable glycerol chemisorption on Ag(111) compared to Pt(111) could be the reason for the low glycerol electro-oxidation rates on Ag electro-catalysts. At low potential, glycerol doesn't adsorb on the Ag(111) surface, whereas at high potential the glycerol electro-oxidation continues all the way to very oxidized products.

4. Summary

In this study, we have explored the catalytic performance for glycerol electro-oxidation on Pt(111) and Ag(111). The initial glycerol adsorption happens via a C* atom on Pt(111) and via an O* atom

on Ag(111). We hypothesize that the different adsorption preference is responsible for the different observed glycerol electro-oxidation product selectivity preference on Pt and Ag catalysts, especially the preference of Ag to break C-C bonds compared to Pt. We identified the most probable oxidation intermediate based on either stability or activation energy at every oxidation step and used this intermediate as the reactant for the next oxidation step. We find that glycerol is most likely oxidized to glyceraldehyde on both surfaces. Glyceraldehyde also adsorbs via a C* atom on Pt(111) and via an O* atom on Ag(111) followed by OH incorporation in the next oxidation state. Due to the different adsorption configurations, the OH incorporation results in glyceric acid (CH₂OH-CHOH-COOH) formation on Pt(111) and C-C bond breaking to formic acid (HCOOH) and glycolaldehyde (CH₂OH-CHO) on Ag(111). The adsorption preference of Pt(111) and Ag(111) is hereby linked to the glycerol electro-oxidation selectivity in accordance with our hypothesis. Our hypothesis, to the extent that it is correct, provides an important design principle for possible glycerol electro-oxidation catalysts, where the general preference of catalysts for breaking C-C bonds can be assessed without much computational effort by identifying the preferred glycerol adsorption configuration. Our hypothesis is also falsifiable, so we hope that other research groups will test its validity by studying relations between preferred adsorption configurations and glycerol electro-oxidation selectivities on a range of electrocatalyst surfaces.

Supporting Information Available

List of products and their abbreviations in the glycerol oxidation reaction, productivities and selectivities of experimental glycerol electro-oxidation reactions with different metal catalysts and reaction conditions, lists of all investigated intermediates in the first, second, third, and fourth oxidation step, NEB reaction pathways for CH₂OH-CHOH-*C=O → *CHOH-CHOH-*C=O + H*

and $\text{CH}_2\text{OH-CHOH-CH}_2\text{OH} \rightarrow \text{CH}_2\text{OH-CHOH-}^*\text{CHOH} + \text{H}^*$ on Pt(111), overview of free energy corrections used to estimate ΔG^{corr}_{eq1} and ΔG^{corr}_{eq2} , and convergence test for the maximum force on each atom used in structure relaxation.

Acknowledgement

The authors gratefully acknowledge financial support from Independent Research Fund Denmark, through grant no 1127-00372B. Z.M., H.H.K., and J.R. also acknowledge the Danish National Research Foundation Center for High-Entropy Alloy Catalysis (CHEAC) DNRF149.

References

- (1) Yang, F.; Hanna, M. A.; Sun, R. Value-Added Uses for Crude Glycerol--a Byproduct of Biodiesel Production. *Biotechnol. Biofuels* **2012**, *5*, 13.
- (2) Ruhal, R.; Aggarwal, S.; Choudhury, B. Suitability of Crude Glycerol Obtained from Biodiesel Waste for the Production of Trehalose and Propionic Acid. *Green Chem.* **2011**, *13*, 3492-3498.
- (3) Leoneti, A. B.; Aragão-Leoneti, V.; de Oliveira, S. V. W. B. Glycerol as a by-Product of Biodiesel Production in Brazil: Alternatives for the Use of Unrefined Glycerol. *Renew. Energy* **2012**, *45*, 138-145.
- (4) Anitha, M.; Kamarudin, S. K.; Kofli, N. T. The Potential of Glycerol as a Value-Added Commodity. *Chem. Eng. J.* **2016**, *295*, 119-130.
- (5) Behr, A.; Eilting, J.; Irawadi, K.; Leschinski, J.; Lindner, F. Improved Utilisation of Renewable Resources: New Important Derivatives of Glycerol. *Green Chem.* **2008**, *10*, 13-30.
- (6) Hu, X.; Lu, J.; Liu, Y.; Chen, L.; Zhang, X.; Wang, H. Sustainable Catalytic Oxidation of Glycerol: A Review. *Environ. Chem. Lett.* **2023**, *21*, 2825-2861.
- (7) Zhang, Z.; Xin, L.; Li, W. Electrocatalytic Oxidation of Glycerol on Pt/C in Anion-Exchange Membrane Fuel Cell: Cogeneration of Electricity and Valuable Chemicals. *Appl. Catal. B* **2012**, *119-120*, 40-48.
- (8) Chen, W.; Zhou, Y.; Shen, Y. Product Distribution of Glycerol Electro-Oxidation over Platinum-Ceria/Graphene Nanosheet. *Electrochemistry* **2019**, *87*, 30-34.
- (9) Kim, H. J.; Kim, Y.; Lee, D.; Kim, J.-R.; Chae, H.-J.; Jeong, S.-Y.; Kim, B.-S.; Lee, J.; Huber, G. W.; Byun, J.; Kim, S.; Han, J. Coproducing Value-Added Chemicals and Hydrogen with Electrocatalytic Glycerol Oxidation Technology: Experimental and Techno-Economic Investigations. *ACS Sustainable Chem. Eng.* **2017**, *5*, 6626-6634.
- (10) Garcia, A. C.; Birdja, Y. Y.; Tremiliosi-Filho, G.; Koper, M. T. M. Glycerol Electro-Oxidation on Bismuth-Modified Platinum Single Crystals. *J. Catal.* **2017**, *346*, 117-124.

- (11) Kwon, Y.; Birdja, Y.; Spanos, I.; Rodriguez, P.; Koper, M. T. M. Highly Selective Electro-Oxidation of Glycerol to Dihydroxyacetone on Platinum in the Presence of Bismuth. *ACS Catal.* **2012**, *2*, 759-764.
- (12) Lee, S.; Kim, H. J.; Lim, E. J.; Kim, Y.; Noh, Y.; Huber, G. W.; Kim, W. B. Highly Selective Transformation of Glycerol to Dihydroxyacetone without Using Oxidants by a PtSb/C-Catalyzed Electrooxidation Process. *Green Chem.* **2016**, *18*, 2877-2887.
- (13) Dai, C.; Sun, L.; Liao, H.; Khezri, B.; Webster, R. D.; Fisher, A. C.; Xu, Z. J. Electrochemical Production of Lactic Acid from Glycerol Oxidation Catalyzed by AuPt Nanoparticles. *J. Catal.* **2017**, *356*, 14-21.
- (14) Qi, J.; Xin, L.; Chadderton, D. J.; Qiu, Y.; Jiang, Y.; Benipal, N.; Liang, C.; Li, W. Electrocatalytic Selective Oxidation of Glycerol to Tartronate on Au/C Anode Catalysts in Anion Exchange Membrane Fuel Cells with Electricity Cogeneration. *Appl. Catal. B* **2014**, *154-155*, 360-368.
- (15) Han, J.; Kim, Y.; Jackson, D. H. K.; Jeong, K.-E.; Chae, H.-J.; Lee, K.-Y.; Kim, H. J. Role of Au-TiO₂ Interfacial Sites in Enhancing the Electrocatalytic Glycerol Oxidation Performance. *Electrochem. Commun.* **2018**, *96*, 16-21.
- (16) Thia, L.; Xie, M.; Kim, D.; Wang, X. Ag Containing Porous Au Structures as Highly Selective Catalysts for Glycolate and Formate. *Catal. Sci. Technol.* **2017**, *7*, 874-881.
- (17) Guima, K.-E.; Alencar, L. M.; da Silva, G. C.; Trindade, M. A. G.; Martins, C. A. 3D-Printed Electrolyzer for the Conversion of Glycerol into Tartronate on Pd Nanocubes. *ACS Sustainable Chem. Eng.* **2018**, *6*, 1202-1207.
- (18) Bambagioni, V.; Bianchini, C.; Marchionni, A.; Filippi, J.; Vizza, F.; Teddy, J.; Serp, P.; Zhiani, M. Pd and Pt-Ru Anode Electrocatalysts Supported on Multi-Walled Carbon Nanotubes and Their Use in Passive and Active Direct Alcohol Fuel Cells with an Anion-Exchange Membrane (Alcohol=Methanol, Ethanol, Glycerol). *J. Power Sources* **2009**, *190*, 241-251.
- (19) Wang, H.; Thia, L.; Li, N.; Ge, X.; Liu, Z.; Wang, X. Pd Nanoparticles on Carbon Nitride-Graphene for the Selective Electro-Oxidation of Glycerol in Alkaline Solution. *ACS Catal.* **2015**, *5*, 3174-3180.
- (20) Han, J.; Kim, Y.; Kim, H. W.; Jackson, D. H. K.; Lee, D.; Chang, H.; Chae, H.-J.; Lee, K.-Y.; Kim, H. J. Effect of Atomic-Layer-Deposited TiO₂ on Carbon-Supported Ni Catalysts for Electrocatalytic Glycerol Oxidation in Alkaline Media. *Electrochem. Commun.* **2017**, *83*, 46-50.
- (21) Kwon, Y.; Schouten, K. J. P.; Koper, M. T. M. Mechanism of the Catalytic Oxidation of Glycerol on Polycrystalline Gold and Platinum Electrodes. *ChemCatChem* **2011**, *3*, 1176-1185.
- (22) Gomes, J. F.; Garcia, A. C.; Gasparotto, L. H. S.; de Souza, N. E.; Ferreira, E. B.; Pires, C.; Tremiliosi-Filho, G. Influence of Silver on the Glycerol Electro-Oxidation over AuAg/C Catalysts in Alkaline Medium: A Cyclic Voltammetry and in situ FTIR Spectroscopy Study. *Electrochim. Acta* **2014**, *144*, 361-368.
- (23) Yan, H.; Yao, S.; Liang, W.; Feng, X.; Jin, X.; Liu, Y.; Chen, X.; Yang, C. Selective Oxidation of Glycerol to Carboxylic Acids on Pt(111) in Base-Free Medium: A Periodic Density Functional Theory Investigation. *Appl. Surf. Sci.* **2019**, *497*, 143661.
- (24) Valter, M.; dos Santos, E. C.; Pettersson, L. G. M.; Hellman, A. Partial Electrooxidation of Glycerol on Close-Packed Transition Metal Surfaces: Insights from First-Principles Calculations. *J. Phys. Chem. C* **2020**, *124*, 17907-17915.
- (25) Valter, M.; Santos, E. C. d.; Pettersson, L. G. M.; Hellman, A. Selectivity of the First Two Glycerol Dehydrogenation Steps Determined Using Scaling Relationships. *ACS Catal.* **2021**, *11*, 3487-3497.
- (26) Hjorth Larsen, A.; Jørgen Mortensen, J.; Blomqvist, J.; Castelli, I. E.; Christensen, R.; Dufak, M.; Friis, J.; Groves, M. N.; Hammer, B.; Hargus, C.; Hermes, E. D.; Jennings, P. C.; Bjerre Jensen, P.; Kermode, J.; Kitchin, J. R.; Leonhard Kolsbjerg, E.; Kubal, J.; Kaasbjerg, K.; Lysgaard, S.; Bergmann Maronsson, J.; Maxson, T.; Olsen, T.; Pastewka, L.; Peterson, A.; Rostgaard, C.; Schiøtz, J.; Schütt, O.; Strange, M.; Thygesen, K. S.; Vegge, T.;

Vilhelmsen, L.; Walter, M.; Zeng, Z.; Jacobsen, K. W. The Atomic Simulation Environment—a Python Library for Working with Atoms. *J. Phys.: Condens. Matter* **2017**, *29*, 273002.

(27) Enkovaara, J.; Rostgaard, C.; Mortensen, J. J.; Chen, J.; Duřak, M.; Ferrighi, L.; Gavnholt, J.; Glinsvad, C.; Haikola, V.; Hansen, H. A.; Kristoffersen, H. H.; Kuisma, M.; Larsen, A. H.; Lehtovaara, L.; Ljungberg, M.; Lopez-Acevedo, O.; Moses, P. G.; Ojanen, J.; Olsen, T.; Petzold, V.; Romero, N. A.; Stausholm-Møller, J.; Strange, M.; Tritsarlis, G. A.; Vanin, M.; Walter, M.; Hammer, B.; Häkkinen, H.; Madsen, G. K. H.; Nieminen, R. M.; Nørskov, J. K.; Puska, M.; Rantala, T. T.; Schiøtz, J.; Thygesen, K. S.; Jacobsen, K. W. Electronic Structure Calculations with GPAW: A Real-Space Implementation of the Projector Augmented-Wave Method. *J. Phys.: Condens. Matter* **2010**, *22*, 253202.

(28) Mortensen, J. J.; Hansen, L. B.; Jacobsen, K. W. Real-Space Grid Implementation of the Projector Augmented Wave Method. *Phys. Rev. B* **2005**, *71*, 035109.

(29) Hammer, B.; Hansen, L. B.; Nørskov, J. K. Improved Adsorption Energetics within Density-Functional Theory Using Revised Perdew-Burke-Ernzerhof Functionals. *Phys. Rev. B* **1999**, *59*, 7413-7421.

(30) Henkelman, G.; Uberuaga, B. P.; Jónsson, H. A Climbing Image Nudged Elastic Band Method for Finding Saddle Points and Minimum Energy Paths. *J. Chem. Phys.* **2000**, *113*, 9901-9904.

(31) Liu, B.; Greeley, J. Decomposition Pathways of Glycerol via C–H, O–H, and C–C Bond Scission on Pt(111): A Density Functional Theory Study. *J. Phys. Chem. C* **2011**, *115*, 19702-19709.

(32) Valter, M.; Busch, M.; Wickman, B.; Grönbeck, H.; Baltrusaitis, J.; Hellman, A. Electrooxidation of Glycerol on Gold in Acidic Medium: A Combined Experimental and DFT Study. *J. Phys. Chem. C* **2018**, *122*, 10489-10494.

(33) Garcia, A. C.; Kolb, M. J.; van Nierop y Sanchez, C.; Vos, J.; Birdja, Y. Y.; Kwon, Y.; Tremiliosi-Filho, G.; Koper, M. T. M. Strong Impact of Platinum Surface Structure on Primary and Secondary Alcohol Oxidation During Electro-Oxidation of Glycerol. *ACS Catal.* **2016**, *6*, 4491-4500.

(34) Wang, Y.; Zhu, Y.-Q.; Xie, Z.; Xu, S.-M.; Xu, M.; Li, Z.; Ma, L.; Ge, R.; Zhou, H.; Li, Z.; Kong, X.; Zheng, L.; Zhou, J.; Duan, H. Efficient Electrocatalytic Oxidation of Glycerol via Promoted OH* Generation over Single-Atom-Bismuth-Doped Spinel Co₃O₄. *ACS Catal.* **2022**, *12*, 12432-12443.

(35) Schlegel, N.; Bagger, A.; Rossmeisl, J.; Arenz, M. Elucidating the Reaction Pathway of Glucose Electrooxidation to Its Valuable Products: The Influence of Mass Transport and Electrode Potential on the Product Distribution. *J. Phys. Chem. C* **2023**, *127*, 18609-18618.

(36) Rossmeisl, J.; Logadottir, A.; Nørskov, J. K. Electrolysis of Water on (Oxidized) Metal Surfaces. *Chem. Phys.* **2005**, *319*, 178-184.

(37) Nørskov, J. K.; Rossmeisl, J.; Logadottir, A.; Lindqvist, L.; Kitchin, J. R.; Bligaard, T.; Jónsson, H. Origin of the Overpotential for Oxygen Reduction at a Fuel-Cell Cathode. *J. Phys. Chem. B* **2004**, *108*, 17886-17892.

(38) Peterson, A. A.; Abild-Pedersen, F.; Studt, F.; Rossmeisl, J.; Nørskov, J. K. How Copper Catalyzes the Electroreduction of Carbon Dioxide into Hydrocarbon Fuels. *Energy Environ. Sci.* **2010**, *3*, 1311-1315.

(39) Heenen, H. H.; Gauthier, J. A.; Kristoffersen, H. H.; Ludwig, T.; Chan, K. Solvation at Metal/Water Interfaces: An Ab Initio Molecular Dynamics Benchmark of Common Computational Approaches. *J. Chem. Phys.* **2020**, *152*.

(40) Verma, A. M.; Laverdure, L.; Melander, M. M.; Honkala, K. Mechanistic Origins of the pH Dependency in Au-Catalyzed Glycerol Electro-Oxidation: Insight from First-Principles Calculations. *ACS Catal.* **2022**, *12*, 662-675.

(41) Garcia-Araez, N. Standard Adsorption Gibbs Energy for Hydrogen, OH, Chloride, and Sulfate on Pt(111): Comparison of Different Isotherms. *J. Phys. Chem. C* **2011**, *115*, 3075-3082.

- (42) Kristoffersen, H. H.; Vegge, T.; Hansen, H. A. OH formation and H₂ adsorption at the liquid water–Pt(111) interface. *Chem. Sci.*, **2018**, *9*, 6912-6921
- (43) Pedersen, J. K.; Clausen, C. M.; Skjægstad, L. E. J.; Rossmeisl, J. A Mean-Field Model for Oxygen Reduction Electrocatalytic Activity on High-Entropy Alloys**. *ChemCatChem* **2022**, *14*, e202200699.
- (44) Peterson, A. A.; Grabow, L. C.; Brennan, T. P.; Shong, B.; Ooi, C.; Wu, D. M.; Li, C. W.; Kushwaha, A.; Medford, A. J.; Mbuga, F.; Li, L.; Nørskov, J. K. Finite-Size Effects in O and CO Adsorption for the Late Transition Metals. *Top. Catal.* **2012**, *55*, 1276-1282.
- (45) Bockris, J. O. M.; Jeng, K. T. In-Situ Studies of Adsorption of Organic Compounds on Platinum Electrodes. *J. Electroanal. Chem.* **1992**, *330*, 541-581.
- (46) Kristoffersen, H. H.; Chang, J. H. Effect of Competitive Adsorption at the Interface between Aqueous Electrolyte and Solid Electrode. *ACS Symp. Ser.* **2019**, *1331*, 225-238.
- (47) Akinola, J.; Barth, I.; Goldsmith, B. R.; Singh, N. Adsorption Energies of Oxygenated Aromatics and Organics on Rhodium and Platinum in Aqueous Phase. *ACS Catal.* **2020**, *10*, 4929-4941.
- (48) Marković, N. M.; Gasteiger, H. A.; Ross, P. N. Oxygen Reduction on Platinum Low-Index Single-Crystal Surfaces in Alkaline Solution: Rotating Ring DiskPt(hkl) Studies. *J. Phys. Chem.* **1996**, *100*, 6715-6721.
- (49) Montemore, M. M.; Medlin, J. W. Predicting and Comparing C–M and O–M Bond Strengths for Adsorption on Transition Metal Surfaces. *J. Phys. Chem. C* **2014**, *118*, 2666-2672.